Computation of Shoaling and Breaking Waves in Nearshore Areas by the Coupling of BEM and VOF Methods *

Stéphan Guignard[1,2], *Stéphan T. Grilli*[3], *Richard Marcer*[2], *and Vincent Rey*[1]

1. LSEET, Upresa 6017 du CNRS, Université de Toulon et du Var, BP 132, 83957 La Garde Cedex, France

2. Principia R&D S.A., Z.I. Bregaillon, 83507 La Seyne-sur-mer Cedex, France

3. Department of Ocean Engineering, University of Rhode Island, Narragansett, RI 02882, USA

ABSTRACT

A numerical wave tank based on the coupling of a Boundary Element model, solving fully nonlinear potential flow equations, and a Volume Of Fluid model solving Navier-Stokes equations is developed and used to calculate transformation of shoaling and breaking waves in nearshore areas.

INTRODUCTION

The Boundary Element Method (BEM) has proved very efficient for calculating the propagation and shoaling of ocean waves over arbitrary bottom topography, up to overturning of a wave (e.g., Grilli *et al.*, 1994, 1997, 1998; Grilli and Horrillo, 1997, 1998). In such computations, fully nonlinear potential flow theory is typically solved in a Boundary Integral formulation based on free space Green's function, coupled to a higher-order time updating of both the boundary geometry and potential. Such numerical models are often referred to in the literature as *numerical wave tanks* (NWT) because they simulate the functionality of laboratory tanks, i.e., wave generation, propagation and radiation/absorption (see below). Many laboratory experiments have shown that computations in NWTs based on potential flow equations are very accurate in predicting both the shape and kinematics of surface waves shoaling over a sloping bottom, up to the breaking point (for which waves have a vertical tangent on the front face), and slightly beyond, up to the instant of impact of a breaker jet on the free surface (e.g., Grilli *et al.*, 1994, 1997). Further than this, however, the method breaks down due to the violation of governing equations.

This limitation of BEM-NWTs to non-breaking waves has led to the development of various artificial methods for preventing breaking in computations. These methods are usually referred to as *absorbing beaches* (AB) (e.g., Cointe, 1990; Clément, 1996; Grilli and Horrillo, 1997, 1998; see Fig. 1). Their principle is to absorb energy from incident waves, at the extremity of the NWT, before they start overturning, through a combination of surface pressure and lateral active absorption ("absorbing pistons", AP). Without an AB, periodic waves shoaling up a slope would normally lead to a succession of breakers at the top of the slope, of which only the first one would be calculated in the NWT. With an AB, however, successive waves can be let to shoal up to very close to the breaking point, before they enter the AB and dissipate their energy (Grilli and Horrillo, 1997, 1998).

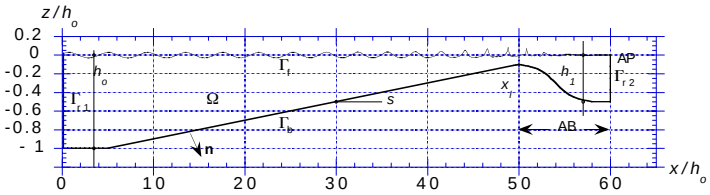

Figure 1 : Sketch of periodic wave shoaling computations over a plane slope s in Grilli and Horrillo's (997) 2D-BEM-NWT, with an absorbing beach (AB) and an absorbing piston (AP) at the extremity.

Note that such ABs are essentially non-physical in the sense that, while globally absorbing wave energy, they do not dissipate energy the way it occurs in nature, i.e., through the combined action of vorticity, turbulence, and viscosity within the fluid volume. Hence, results for wave shape and kinematics are useless within the AB, which can only be regarded as a "black box" performing an energy absorption function in a numerical model.

Constant improvements in computer power have recently led

*In *Proc. 9th Offshore and Polar Engng. Conf.* (ISOPE99, Brest, France, May 1999), Vol. III, 304-309.

These methods directly solve the complete Navier-Stokes equations on a grid covering the whole domain, and are able to accurately follow the motion of free surfaces and interfaces between fluids, by using distributed Lagrangian surface markers. VOF methods allow for pockets of air to be trapped within the fluid domain and for pieces of water to detach from the main computational domain. Hence, these methods are ideally suited for modeling breaking waves over a sloping bottom [e.g., Guignard *et al.*, 1998, 1999; Fig. 2; note, however, in this model, the air-phase is assumed to be incompressible, even for pockets of air trapped in the water : this may be an approximation for violent impulsive problems.]. VOF methods, however, are computationally expensive and suffer from numerical diffusion, leading to artificial loss of wave energy over long distances of propagation.

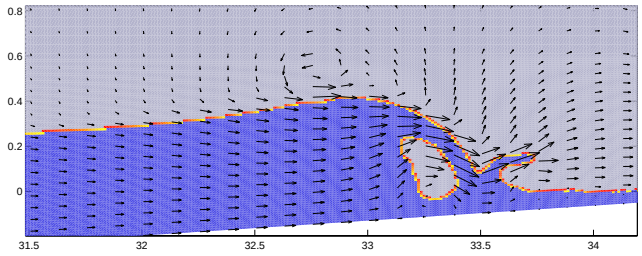

Figure 2 : Breaking of a solitary wave over a 1:15 slope in a two-phase VOF model [Guignard *et al.*, 1998]. Light grey represents the air region and dark grey the water region. Arrows indicate flow velocities.

In the present study, the key features and advantages of both BEM and VOF methods are exploited, by coupling these methods to carry out wave shoaling computations further than the impact of a breaker jet on the free surface. The BEM method, implemented into a NWT with an AB, accurately and efficiently models wave shoaling over a sloping bottom, before breaking occurs. The VOF method can calculate breaking and post-breaking waves at the top of the sloping bottom, on a refined local grid, with fluid flow parameters being both initialized and updated at the open ocean boundary, using the BEM-NWT. The coupled model allows for efficient and accurate computations of nearshore wave propagation and transformation.

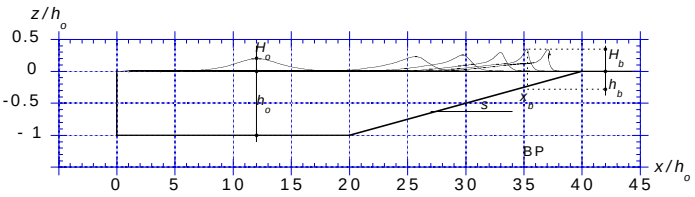

Figure 3 : Shoaling and overturning of a solitary wave of height [as in Grilli *et al.*, 1997]

In the present paper, BEM/VOF model coupling is only realized for solitary waves shoaling and breaking over mild slopes, for which little reflection occurs (e.g., Fig. 3). This is the simplest case in which no feed back occurs from the VOF model into the BEM model. More complex cases with periodic waves and feed back are in progress and will be presented at the conference.

NUMERICAL MODELS

BEM MODEL

Grilli *et al.* (1989), and Grilli and Subramanya (1996) implemented an efficient and accurate two-dimensional (2D) BEM model solving fully nonlinear potential flow equations (FNPF; Fig. 1), continuity equation,

$$\nabla^2 \phi = 0 \qquad \text{in } \Omega(t) \tag{1}$$

the fully nonlinear kinematic and dynamic free surface boundary conditions,

$$\frac{D\mathbf{r}}{Dt} = \left(\frac{\partial}{\partial t} + \mathbf{u}\cdot\nabla\right)\mathbf{r} = \mathbf{u} = \nabla\phi \qquad \text{on } \Gamma_f(t) \tag{2}$$

$$\frac{D\phi}{Dt} = -gz + \frac{1}{2}\nabla\phi\cdot\nabla\phi - \frac{p_a}{\rho} \qquad \text{on } \Gamma_f(t) \tag{3}$$

respectively, with $\mathbf{r}$, the position vector on the free surface, g the gravitational acceleration, z the vertical coordinate, p_a the pressure at the free surface, and ρ the fluid density; and a no-flow condition on the bottom,

$$\overline{\frac{\partial\phi}{\partial n}} = 0 \qquad \text{on } \Gamma_b \tag{4}$$

where the overline denotes specified values. Boundary conditions on lateral boundaries Γ_{r1} and Γ_{r2} are discussed next.

Grilli and Horrillo (1997) implemented accurate generation and absorption of periodic waves in this BEM model and developed it into a 2D-NWT applicable to shoaling waves. More specifically their NWT combined : (i) a higher-order BEM solution of Fully Nonlinear Potential Flow (FNPF) equations; (ii) an exact generation of finite amplitude periodic waves (*Streamfunction Waves*) at the deeper water extremity (Γ_{r1}); and (iii) an *Absorbing Beach* (AB) at the far end of the tank (featuring both free surface absorption on Γ_f and lateral active absorption on Γ_{r2}; Fig. 1). Applications showed that, after absorption of initial transient waves, computations in this NWT reached a *quasi-steady* state for which reflection from the AB was very small. Details can be found in the above-referenced papers.

VOF MODEL

Guignard *et al.* (1998,1999) developed a numerical model for simulating multi-interface two-phases (air/water) viscous incom-

Stokes equations in both fluids, with respect to their real density (pseudo-compressibility method; e.g., Viviand, 1995; Laget 1998). A curvilinear grid with variable mesh, covering both fluids, is defined along the x and z directions. Interfaces and their motion are time-updated using a new Lagrangian method referred to as SL-VOF method (Guignard *et al.*, 1998). In this method, interfaces are modeled two ways : (i) a *color* function is defined within each cell of the VOF grid, as the fraction (0 to 1) of the cell area occupied by the denser fluid (classical VOF concept); hence, any fraction less than one in a cell indicates the presence of an interface in this cell; (ii) a segmental representation of the interface is defined based on the values of the color function, according to a Peacewise Linear Interface Calculation concept (e.g., Li 1995).

Interface segments are advected as a function of time, following the velocity field obtained from the VOF solution of Navier-Stokes equations. After this advection, new values of the color function are computed, taking into account the new position of the segments. Details can be found in the above-referenced papers.

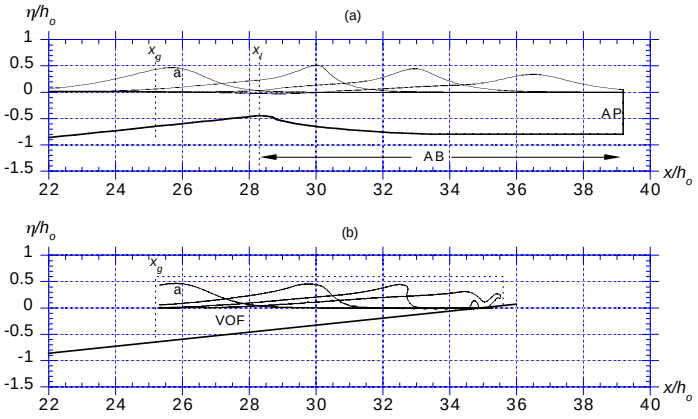

Figure 4 : Principle of BEM/VOF model coupling. (a) Shoaling and absorption in the BEM-NWT with an AB (and an AP) starting at x_l', of a solitary wave with incident height H_o/h_o, over a mild plane slope. Fluid velocities and pressures are calculated at a vertical gage at x_g. (b) Same computations in the VOF model, initialized with wave a, and using lateral boundary conditions at x_g from part (a).

PRINCIPLE OF COUPLED MODEL

Grilli *et al.*'s 2D-NWT described above models the propagation of arbitrary fully nonlinear waves over complex bottom topographies. Boundary values of wave flow parameters (velocity, acceleration, pressure,...) are readily available in the results; if needed, values of the same fields can also be computed at specified interior points. Guignard *et al.* (1998) used this NWT to generate initial data in their VOF model, for the propagation of large solitary waves in constant depth and over a slope. In sults, particularly over long distances of propagation, are affected by numerical diffusion which leads to an artificial decrease in energy and wave elevation as the wave propagates. Also, because of the large fluid domain, such VOF computations are extremely demanding in terms of computer resources. In fact, these computations could only be performed in a reasonable CPU time by using several sub-domains, with large overlapping parts, and independently calculating the propagation of solitary waves in these sub-domains, from one sub-domain to the next one.

In the present paper, in what is referred to as *weak coupling*, the BEM-NWT is used, as in Grilli *et al.* (1997), to calculate the propagation of a solitary wave over a mild slope, up to close to the breaking point (BP, Figs. 3 and 4a). Here, however, to prevent wave overturning, an AB is specified at the upper part of the slope. BEM results, calculated along a vertical line as a function of time, are then used as open ocean boundary conditions in the VOF model (Fig. 4b).

More specifically, a first computation is run in the NWT without the AB (e.g., Fig. 5a), up to a crest location close to the BP (curve a), and field values are calculated at internal points corresponding to the VOF model grid mesh centers. These values are used as initial fields in VOF computations (e.g., Fig. 4b). A second computation is then run in the NWT, for the same wave, using the AB to absorb incident wave energy (e.g., Fig. 4a, 5b). In this case, a numerical wave gage is specified close to the entrance of the beach, at which both boundary and internal field values are calculated, at the vertical locations of VOF grid centers, and saved as a function of time. These time series of velocity, pressure, and wave elevation are finally used in the VOF model as lateral boundary conditions (e.g., Fig. 6).

By proceeding this way, the capabilities of both BEM and VOF methods are combined at best. Initial wave fields and upstream lateral boundary values calculated in the NWT and specified in the VOF model are not affected by numerical diffusion. The VOF model, in turn, only operates over short propagation distances and hence, provides both accurate and efficient results for post-breaking waves, which are beyond the reach of the BEM-NWT. More details, values of model parameters, and results, are given in the next section.

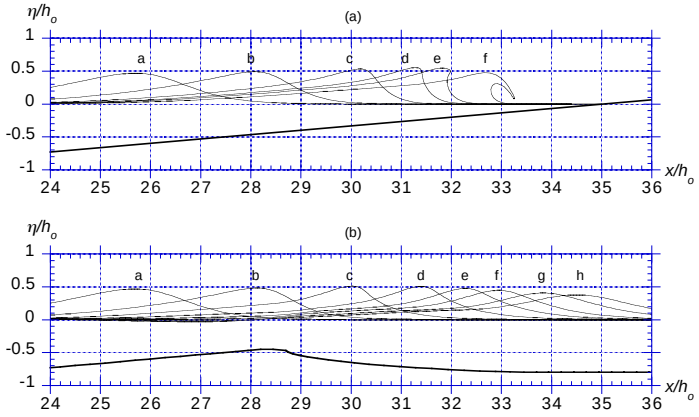

Figure 5 : Shoaling and breaking of a solitary wave with $H_o/h_o =$

measured from the point the incident wave crest is at $x' = x/h_o =$ 25.67, i.e., t' =a: 0, b: 1.81, c: 3.44, d: 4.78, e: 5.72, f: 6.51, g: 7.22, h: 7.89.

Let us finally point out that the term *weak coupling* refers to the fact that, in the present case, both models are independently run. Hence, although BEM-NWT results are fed into the VOF model, there is no feed back from this model to the BEM-NWT. We will see that, for solitary waves, this in fact does not affect results at all. For periodic waves, however, which will be used in a second stage, feed back will be necessary and will require the implementation of a *strong coupling* algorithm.

MODEL VERIFICATION AND RESULTS

SHOALING OF SOLITARY WAVES IN BEM AND VOF MODELS

As mentioned before, only results for solitary waves shoaling and breaking over a mild slope are presented in this paper. The set-up for the corresponding BEM-NWT computations is given in Fig 3. A fully nonlinear solitary wave is used as incident wave (i.e., a solution of FNPF equations), with an initial height $H_o = 0.45\, h_o$ in depth $h_o = 1$; a mild 1/15 slope is specified in the NWT. This is the same case as used in Guignard *et al.* (1998). This solitary wave is first specified in the NWT without an AB, at $x' = x/h_o = 12$ (dashes indicate dimensionless variables), using its shape and kinematics calculated with Tanaka's (1986) method—as implemented and used by Grilli *et al.* (1994,1997) to study solitary wave propagation over slopes—. The boundary of the NWT is discretized using 452 nodes, 300 of which are located on the free surface of length $34.4h_o$. The initial horizontal spacing between free surface nodes is, $\Delta x'_o = \Delta x_o/h_o = 0.115$, and the initial dimensionless time step in the BEM model is $\Delta t'_o = \Delta t\sqrt{g/h_o} = 0.045$; this corresponds to a mesh Courant number of $\Delta t'_o/\Delta x'_o = 0.4$.

All the computations in this work were performed on a DEC Alpha 500 workstation. With the above data the BEM model requires 3.4s CPU time per time step. Fig. 5a shows results of these computations at 6 successive times, with corresponding free surface shapes denoted by curves a to f. As the wave shoals up, due to convergence of BEM nodes towards the wave crest, the time step adaptively decreases in the model, in order to maintain a constant mesh Courant number (see Grilli and Subramanya, 1996). It takes 260 time steps for the wave to reach the location of curve a in the NWT from its initial location, and another 600 steps to reach the location of curve f. Hence, the total CPU time is

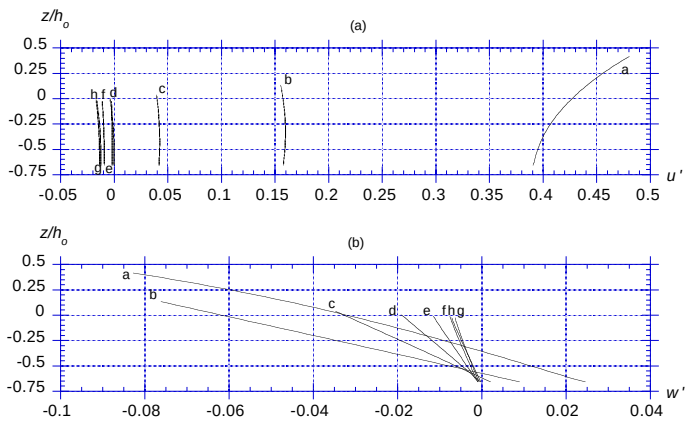

Figure 6 : Same case as in Fig. 5. Dimensionless particle velocities calculated in the BEM-NWT with the AB (Fig. 5b), over a vertical gage at $x'_g = 25.67$, from bottom to surface (Fig. 4) : (a) horizontal velocities; (b) vertical velocities.

The same computation is repeated in the NWT with an AB starting at $x'_l = 28.4$ (with an AP at the rightward extremity). The bottom geometry is modified for $x' > x'_l$, as shown in Fig. 4a, in order to help the AB absorb wave energy by creating some de-shoaling in the wave. In this second computation, the NWT is initialized at the time of curve a in Fig. 5a, using results obtained in the NWT without the AB. The boundary of the NWT is discretized using 500 nodes, 344 of which are located on the free surface of length $39.2h_o$. The initial horizontal spacing between free surface nodes is $\Delta x'_o = 0.114$ and the initial time step in the BEM model is $\Delta t'_o = 0.045$; this again corresponds to a mesh Courant number of 0.4. With these data the BEM model requires 4.2s CPU time per time step. Fig. 5b shows results of these computations at 8 successive times, with corresponding free surface shapes denoted as curves a to h. At each time step, velocities, pressure and surface elevation are calculated at (80) equally spaced locations, from bottom to surface, along a numerical gage located at $x'_g = 25.67$ (Fig. 4a). These will be used as lateral upstream boundary conditions in the VOF model.

Comparing results in Fig. 5b with those in Fig. 5a, one can see that the AB does not affect wave propagation for $x' < x'_l$. Wave height, however, gradually decreases within the AB as energy absorption occurs. This makes it possible to keep computing solitary wave propagation for a longer time then without the AB, much beyond the stage of curve e in Fig. 5a, for which NWT computations without an AB break down. Hence, flow parameters at $x' = x'_g$ are available for a longer time, allowing the VOF computations to be pursued into the post-breaking regime (see next Section). Fig. 6, for instance, shows dimensionless horizontal and vertical velocities $u' =$

h (Fig. 5).

BREAKING SOLITARY WAVES IN COUPLED MODEL

As shown in Fig. 4b, the VOF model is run over a smaller computational domain than the BEM-NWT, extending from $x' = x'_g$ to the upper part of the slope in the horizontal direction at $x' = 35.6$, and from the slope solid boundary to $z' = 0.6$, in the vertical direction. Computations are initialized using BEM-NWT results corresponding to curve a in Fig. 5a

In the VOF computations, 825 equally spaced grid points are used in the horizontal direction, with mesh size $\Delta x' = 0.012$, and 80 grid points are used in the vertical direction, with mesh size gradually decreasing towards the top of the slope, from $\Delta z' = 0.0153$ at $x' = x'_g$. The time step in the VOF computations is adaptively selected to maintain the mesh Courant number to a value smaller than 0.9 (Guignard *et al.*, 1998). The BEM-NWT is used to calculate initial internal values of velocity and pressure at the 825x80 grid points of the VOF model. With these data, the initial time step is selected to $\Delta t'_o = 0.020$ and the CPU time required to compute a time step is 232s, i.e., about 68 times as much as computations in the BEM-NWT without an AB for the same case. For later times, the time step gradually decreases to reach 0.005 at the end of the VOF computations. About 750 time steps are thus required to propagate the wave from curve a to h in the coupled VOF model. Hence, the total computation time is about 48h on the DEC Alpha 500.

After initialization of the VOF model as explained above, computations are carried out using velocities (Fig. 6) and pressure calculated at the lateral upstream boundary, in the BEM-NWT with the AB. Results are given in Fig. 7b, as compared to results obtained in the BEM-NWT over the same area, shown in Fig. 7a as a reference. Note that these BEM results have been compared to high resolution laboratory experiments by Grilli *et al.* (1994,1997), who found that maximum differences were only 1-2%, up to the breaking point. More recently, details of the jet calculated in the BEM-NWT for a stage close to curve e were experimentally validated by Li and Raichlen (1998) (see also Grilli *et al.*, 1998). Hence, results from the BEM-NWT can be considered as very accurate in this case and any major discrepancy of VOF results up to, say, the stage of curve d should mostly be due to computational errors.

In fact, comparing curves b and c in Figs. 7a and b, we see that both results are quite similar with, however, a small reduction in wave height for curve c in VOF computations as compared to BEM results. In light of the above discussion, this reduction in height should mainly be the result of numerical diffusion in the VOF algorithm and not (yet) of

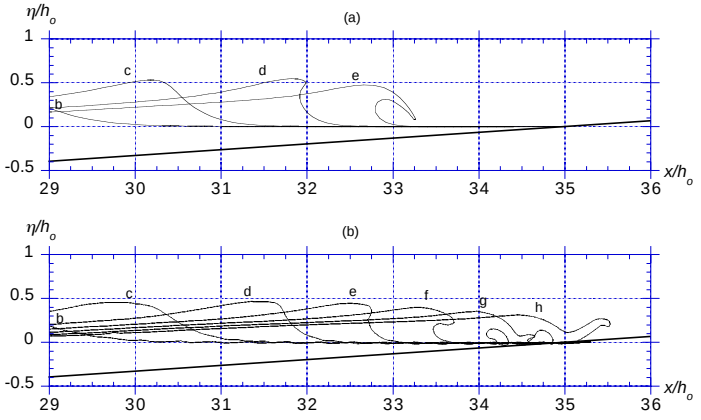

Figure 7 : Same case as in Fig. 5, calculated in : (a) the BEM-NWT (same as Fig. 5a); and (b) the *weakly coupled* VOF model. Computations are initialized in the VOF model at the time of curve a and boundary conditions are specified at $x/h_o = 25.67$, using the BEM-NWT.

Due to this reduction in height, for later times (curves d-e), the wave propagates slightly slower in the VOF model and the breaker jet also develops slower, and thus occurs slightly later, than in BEM computations.

Beyond the stage of curve e, the breaker jet impacts the free surface and the slope. Hence, BEM computations without an AB break down and results for these times are only available in the VOF model. Due to the impact of the jet on the slope, in the latter model, the jet quite realistically rebounds forward while a pocket of air is enclosed within the breaking wave.

As mentioned above, Guignard *et al.* (1998) carried out computations for the same wave propagating in a larger VOF domain divided into several overlapping parts. The last such part extended from $x' = 10$ to 35.6 (Fig. 3) and used 1800 and 80 grid points in the horizontal and vertical directions, respectively, with $\Delta x' = 0.014$, and $\Delta z'$ reducing from 0.02 in constant depth $h_o = 1$. The CPU time required to compute a time step in this grid was 506s. Despite a slightly smaller resolution and a significantly larger computational time, Guignard *et al.* were able to calculate wave breaking up to the stage of curve h in Fig. 7b (e.g., Fig. 2). The loss in wave height, however, was larger than in present computations, due to numerical diffusion effects occurring over longer distances of propagation. A comparison with laboratory experiments confirmed that the VOF model underestimated wave heights.

In view of the above results, we see that the weakly coupled VOF model is both more accurate and efficient than the VOF model used alone over a larger grid. Due to the re-

even more accurate.

CONCLUSIONS

A coupled BEM/VOF model was developed which combines at best the features and advantages of Boundary Element and Volume Of Fluid methods. At this stage, only solitary waves shoaling and breaking over plane slopes were used, and a *weak* coupling algorithm, i.e., without any feed-back from the VOF to the BEM model, was specified.

Due to its better numerical accuracy and efficiency for non-breaking waves, the BEM model is used to carry out most of the wave propagation from open waters to the upper slope, up to close to the breaking point. VOF computations of similar resolution are at least 50 times slower, and can be affected by numerical diffusion. Model coupling then occurs at two levels : (i) the VOF model is initialized over a smaller area than that covered by the BEM model, using BEM results calculated over the VOF grid; (ii) for later times, the lateral upstream boundary condition in the VOF model is provided by BEM results calculated over a vertical gage. To be able to pursue computations for a sufficiently long time in the BEM model, an absorbing beach is used at the top of the slope to prevent wave overturning and breaking.

In this approach, the BEM and VOF models are thus essentially run in sequence. Both, initial values, and a data base of lateral boundary conditions as a function of time, are calculated and saved in the BEM model. The VOF model is then run. This is why this situation is referred to as *weak coupling*.

By contrast, in recent developments, a *strong coupling* algorithm is being developed in which both BEM and VOF models will be simultaneously run, one model providing open boundary conditions for the other one, and *vice-versa*, over a vertical matching boundary defined at a similar location as $x = x_g$ in the present case. In this *strong coupling* algorithm, more complex cases with, e.g., periodic waves or wave groups will be within reach of VOF computations, which will make it possible to gain new physical insight into the breaking and post-breaking of these more complex wave trains.

ACKNOWLEDGMENT

This paper is collaborative work carried out at the LSEET laboratory, Upresa 6017 du CNRS, Université de Toulon et du Var, France, while the second author was an invited professor on sabbatical leave from the University of Rhode Island, USA. LSEET's material support for this research is gratefully acknowledged.

Clément, A. (1996) Coupling of Two Absorbing Boundary Conditions for 2D Time-domain Simulations of Free Surface Gravity Waves. *J. Comp. Phys.,* **126,** 139-151.

Cointe, R. (1990) Numerical Simulation of a Wave Channel. *Engng. Analysis with Boundary Elements,* **7**(4), 167-177.

Grilli, S.T. and Horrillo, J. (1997) Numerical Generation and Absorption of Fully Nonlinear Periodic Waves. *J. Engng. Mech.,* **123**(10), 1060-1069.

Grilli, S.T. and Horrillo, J. (1998) Computation of periodic wave shoaling over barred-beaches in a fully nonlinear numerical wave tank. In Proc. ISOPE98 (Montreal, Canada, May 1998) (eds. Chung, J.S., Olagnon, M., Kim, C.H., Koterayama, W.), Vol. III, pps. 294-300.

Grilli, S.T. and Horrillo, J. (1999) Computation of properties of periodic waves shoaling over mild slopes in a fully nonlinear numerical wave tank. *J. Geophysical Res.* (submitted).

Grilli, S.T., Skourup, J., and Svendsen, I.A. (1989) An efficient boundary element method for nonlinear water waves. *Engng. Analysis with Boundary Elements,* **6**(2), 97-107.

Grilli, S.T. and Subramanya, R. (1996) Numerical modeling of wave breaking induced by fixed or moving boundaries. *Computational Mech.,* **17**, 374-391.

Grilli, S.T., Subramanya, R., Svendsen, I.A., and Veeramony, J. (1994) Shoaling of Solitary Waves on Plane Beaches. *J. Waterways Port Coastal Ocean Engng.,* **120**(6), 609-628.

Grilli, S.T., Svendsen, I.A., and Subramanya, R. (1997) Breaking Criterion and Characteristics for Solitary Waves on Slopes. *J. Waterways Port Coastal Ocean Engng.,* **123**(3), 102-112.

Grilli, S.T., Svendsen, I.A. and Subramanya, R. (1998) Breaking Criterion and Characteristics for Solitary Waves on Slopes – Closure. *J. Waterway Port Coastal Ocean Engng.,* **124**(6), 333-335.

Guignard, S., Marcer, R., Rey, V., Kharif, Ch., and Fraunié, Ph. (1998) Solitary Wave Breaking on Sloping Beaches : 2D two-phase Flow Numerical Simulation by SL-VOF Method. *Eur. J. Mech.* (submitted).

Guignard, S., Marcer, R. and Rey, V. (1999) New VOF Method for Simulation of Nonlinear Wave Effects. To appear in *Proc. ISOPE99 Conf.* (Brest, France).

Hirt and Nicholls (1981) Volume of Fluid Method for the Dynamics of Free Boundaries. *J. Comp. Phys.,* **39,** 323-345.

Laget, 0. (1998) Résolution des équations d'Euler pour les écoulements non-linéaires en présence d'une interface. *Thèse de doctorat.* Université de Nice-Sophia Antipolis.

Li, J. (1995) Piecewise Linear Interface Calculation. *C. R. Acad. Sci. Paris,* **320** (II b), 391-396.

Li, Y., and Raichlen, F. (1998) Breaking criterion and characteristics for solitary waves on slopes – Discussion. *J. Waterway Port Coastal Ocean Engng.,* **124**(6), 329-333.

Tanaka, M. (1986) The Stability of Solitary Waves. *Phys. Fluids,* **29,** 660-665.

Viviand, H. (1995) Analysis of pseudo-compressibility systems for compressible and incompressible flows. *Comp Fluid. Dynamics Rev.* **29**(3), 650-655.